

AN OCCURRENCE OF SAPPHIRINE IN THE ARCHEAN SUPERIOR PROVINCE, NORTHERN QUEBEC

SANDRINE CADÉRON[§]

Ministère des Ressources Naturelles du Québec, 400 Boulevard Lamaque, Bureau 1.02, Val-d'Or, Québec J9P 3L4, Canada

WALTER E. TRZCIENSKI JR.

Département de Géologie, Université de Montréal, 2900, boulevard Edouard Montpetit, Montréal, Québec H3T 1J4, Canada

JEAN H. BÉDARD

Commission Géologique du Canada, C.P. 7500, Ste-Foy, Québec G1V 4C7, Canada

NORMAND GOULET

*Département des Sciences de la Terre et de l'Atmosphère, Université du Québec à Montréal,
201 Président Kennedy, Montréal, Québec H2X 3Y7, Canada*

ABSTRACT

A clast containing sapphirine has been found in the Troie Complex in the Archean Minto Subprovince, in the northeastern part of the Superior Province, in northern Quebec. The area is dominated by synmagmatically deformed felsic plutonic rocks that host volcano-sedimentary slivers and rafts. The Douglas Harbour Domain contains the Faribault–Thury tonalite–trondhjemite complex, intruded by the 2740–2726 Ma enderbitic Troie Complex. Slivers and enclaves of volcano-sedimentary rocks in the Troie Complex are metamorphosed to granulite grade. A breccia in the core of the Troie Complex contains a heterogeneous population of xenoliths in an enderbitic matrix. The clast contains sapphirine as symplectitic rims with plagioclase or K-feldspar (or with both) developed around sillimanite and cordierite. Sapphirine also forms a corona around green hercynite, with K-feldspar rimming the sapphirine. Reaction textures, annealing and polygonization indicate localized equilibration, with mosaic equilibrium preserved on the thin-section scale. Various geothermobarometers yield estimates of high temperatures (755–1260°C) and pressures (7.5–14 kbar). The existence of localized equilibria is difficult to interpret in terms of simple prograde or retrograde metamorphism linked with orogenesis. Either static P–T conditions for a protracted period, or minimal attainment of granulite-facies conditions are required to produce and preserve these mosaic textures.

Keywords: Archean, sapphirine, thermobarometry, granulite, metasedimentary rocks, enderbite, Superior Province, Minto Subprovince, Douglas Harbour Domain, Quebec.

SOMMAIRE

Nous avons découvert un fragment de brèche contenant la sapphirine dans le Complexe de Troie dans la Sous-province archéenne de Minto, au nord-est de la Province du Supérieur, dans le nord du Québec. La géologie régionale comprend des roches plutoniques felsiques comagmatiques contenant des enclaves volcano-sédimentaires. Le Domaine de Douglas Harbour, composé du complexe à tonalite–trondhjemite de Faribault–Thury, se retrouve en intrusion à l'intérieur du complexe enderbitique de Troie, daté à 2740–2726 Ma. Les ceintures et les enclaves des roches volcano-sédimentaires retrouvées dans le Complexe de Troie sont métamorphosées au faciès granulite. Au coeur de ce complexe, une brèche contient une population hétérogène de xénolites dans une matrice enderbitique. Le fragment étudié contient une intercroissance symplectitique de sapphirine avec plagioclase ou avec feldspath potassique (ou bien les deux) qui entoure des cristaux de sillimanite et de cordiérite. La sapphirine forme également une texture coronitique dont le coeur est composé de spinelle vert foncé, entouré de sapphirine, le feldspath potassique formant la dernière couronne. Les réactions observées à partir des différentes textures témoignent d'un équilibre localisé à l'échelle de la lame mince. Différents géothermobaromètres permettent d'estimer des températures (755–1260°C) et pressions élevées (7.5–14 kbar) pour ces assemblages. Ces équilibres localisés sont difficiles à interpréter en tant que

[§] E-mail address: sandrine.caderon@mrnfp.gouv.qc.ca

métamorphisme prograde ou rétrograde en relation avec la tectonique régionale. La formation et la préservation de ces textures en mosaïques nécessitent le maintien de conditions P–T statiques sur une période prolongée ou des conditions P–T minimales au faciès granulite.

(Traduit par la Rédaction)

Mots-clés: Archéen, sapphirine, thermobarométrie, granulite, métasédiments, enderbite, Province du Supérieur, Sous-province de Minto, Domaine de Douglas Harbour, Québec.

INTRODUCTION

Reconstructing the metamorphic evolution of granulitic terranes is generally difficult because of inherent uncertainties regarding determinations of pressure and temperature using geothermobarometers, especially where re-equilibration has occurred during cooling. Sapphirine is a rare mineral that is typically used to infer the development of very high temperatures and pressures (Arima & Barnett 1984, Droop 1989, Hensen & Harley 1990, Bertrand *et al.* 1991, Mohan & Windley 1993, Harley 1998, Harley & Motoyoshi 2000). We report here on a sapphirine-bearing metasedimentary xenolith in an enderbite (pyroxene tonalite) plutonic complex from the Archean Minto Block, in the Superior Province in northern Quebec). The rock contains the assemblage sapphirine + hercynite + sillimanite + cordierite + feldspar, and provides new constraints for the pressure–temperature history of this area. Our objectives are to 1) document the petrology and mineral compositions of this sapphirine occurrence, 2) discuss its textural evolution and estimate the pressure–temperature conditions of its formation, and 3) review the implications of these data for the tectonic evolution of this part of the Archean craton.

GEOLOGICAL SETTING

The Minto Block, in the northeastern Superior Province in Quebec (Fig. 1), is principally composed of Archean felsic plutonic rocks in which are embedded numerous supracrustal slivers or belts (Percival *et al.* 1997). The supracrustal rocks are generally metamorphosed to the amphibolite or granulite facies, with rare preservation of prograde greenschist assemblages in the cores of the largest belts (Percival & Skulski 2000, Bédard *et al.* 2003). The sapphirine-bearing assemblage was discovered in the Douglas Harbour Domain, situated in the northeastern part of the Minto Block.

The Douglas Harbour Domain: the Troie Complex

New mapping, together with geochronological, mineralogical and whole-rock major, trace-elements, and isotopic data (Madore *et al.* 1999, Bédard 2003, Bédard *et al.* 2003), allow definition of three principal Archean lithotectonic complexes within the Douglas Harbour Domain: the Troie and Qimussinguat complexes (TC

and QC, respectively), and the Faribault–Thury Complex (FTC) (Figs. 1, 2). These data have also led to the discovery of numerous supracrustal belts and rafts. Amphibolite-grade belts occur in the FTC, whereas granulite-grade belts occur in the TC and QC (Madore *et al.* 1999). The TC and QC are ovoid massifs dominated by pyroxene + magnetite + biotite enderbite (orthopyroxene-bearing tonalite and trondhjemite). The TC enderbite has yielded U–Pb zircon and SHRIMP ages of 2740 ± 11 – 8 Ma and 2726 ± 8 Ma, with possible inherited cores at 2800–2830 Ma, and a monazite U–Pb age of metamorphism of 2707 ± 3 Ma (Madore *et al.* 1999, Percival *et al.* 2001).

The enderbite suite occurs as massive, rather homogeneous intrusive bodies that show little or no modal or textural variation over many kilometers, and as interlayerings of melanocratic and leucocratic enderbite. Enderbites generally have a north-striking foliation and subvertical lineation. The enderbites of the TC typically contain antiperthitic plagioclase, characterized by serrated grain-boundaries. In the least-deformed facies, feldspar grains are euhedral and quartz is interstitial, suggestive of an igneous origin. Orthopyroxene and clinopyroxene generally form euhedral prisms, but clinopyroxene also may be interstitial to orthopyroxene. Minor green hornblende rims the clinopyroxene. Reddish biotite and large grains of magnetite are ubiquitous and abundant. Minor apatite and zircon are common. Geothermometry indicates magmatic temperatures as high as 1045°C during emplacement, with early crystallization of plagioclase resulting from a low activity of H₂O (Bédard 2003).

Belts of supracrustal rocks in the TC are disrupted, forming disconnected slivers and xenoliths (Fig. 2). In the TC supracrustal belts, the association of metabasalt with metakomatiite, marble, metasandstone, iron formation, felsic tuff, pelite and rare conglomerate, suggest a platformal association (Ayres & Thurston 1985). Mineral assemblages in the metabasic and metapelitic rocks imply granulite-grade conditions (Madore *et al.* 1999, Percival & Skulski 2000).

Large, north-trending sheets of late to post-kinematic porphyritic monzonite and granite cut the TC enderbites, and one of these yielded an average Pb–Pb zircon age between 2680 and 2720 Ma (Madore *et al.* 1999). Coeval hornblende- and mica-bearing gabbro-norite and diorite intrusions of shoshonitic affinity are common (Madore *et al.* 1999).

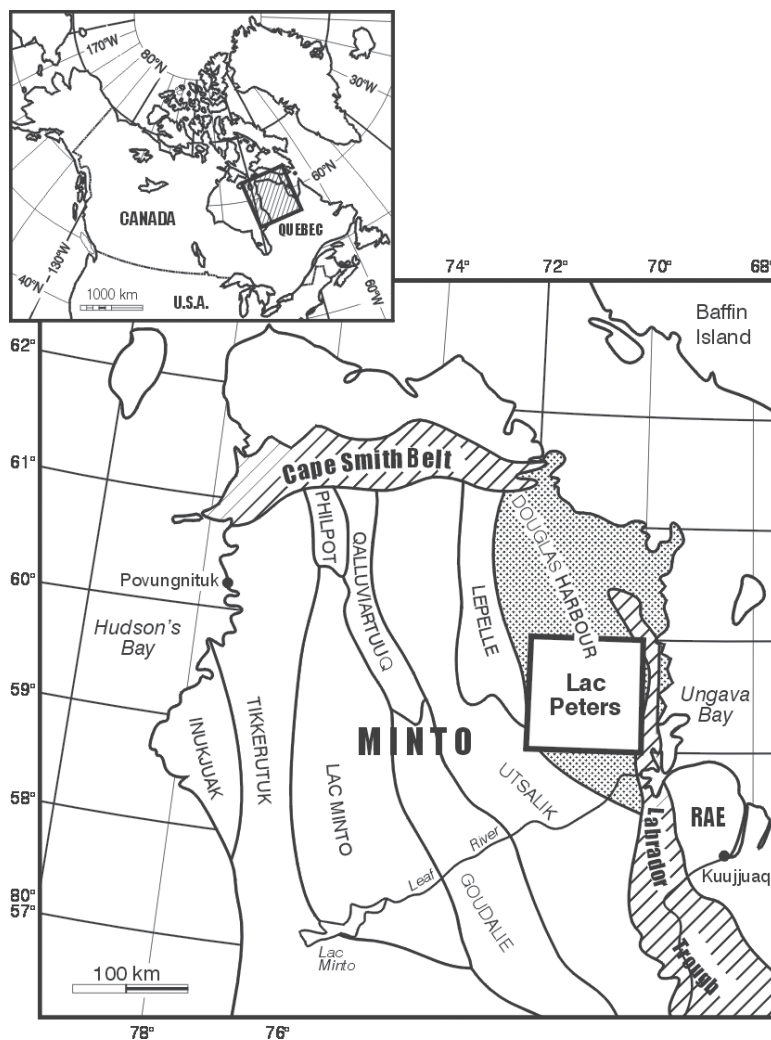


FIG. 1. Location of the Lac Peters study area in the Troie Complex.

PETROGRAPHY

Sample selection

During a 1/250,000 scale mapping traverse, a number of samples were taken from a heterolithic igneous breccia characterized by angular xenoliths (1–5 m, Fig. 2) of hornblende gabbro-norite (65%), enderbite augen gneiss (15%) and metapelite (10%). One of these xenoliths was sampled (Fig. 2) because of the presence of centimetric dark blue prisms in a dark grey-green leuco-enderbite matrix; it was recognized as sapphirine after the fieldwork. This clast could have been a metapelite

or an altered igneous rock composed of chlorite and clays which, once metamorphosed, gave the observed assemblages. Compositional layering at the thin-section scale is defined by layers rich in cordierite + feldspar + quartz locally with rich patches of biotite intercalated with similar bands dominated by sapphirine. The lack of detailed field-work in this area leaves certain aspects of this occurrence problematic. From the protolith perspective, the process could be one of silicification or, more correctly, granitization. Even without detailed field-based observations, this is the first investigation of the genesis of sapphirine in the Superior craton, and provides important P–T estimates for this segment of the crust.

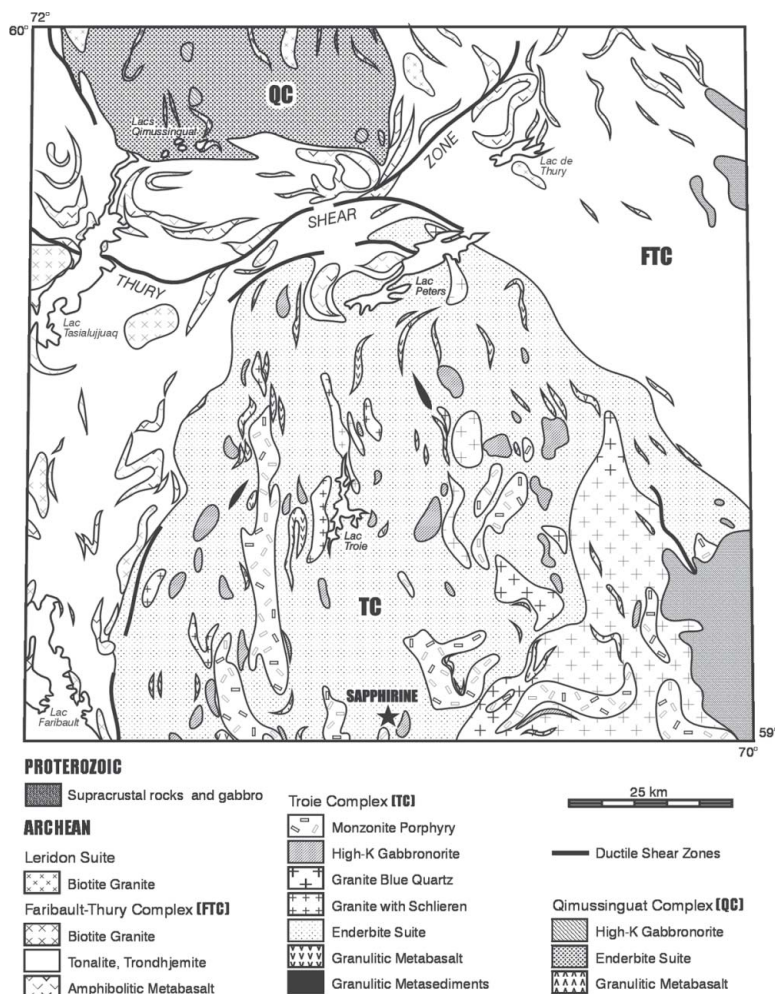


Fig. 2. Geological map of the Lac Peters area (modified from Madore *et al.* 1999).

Petrographic study

Quartz occurs as anhedral microcrystalline grains (<200 μm in size; Fig. 3). It is in contact with altered biotite, K-feldspar and, locally, with hercynite.

Pale blue sapphirine (30%) occurs in two textural habits (Fig. 3). It forms a corona surrounding spinel that is then rimmed by K-feldspar. This corona texture also occurs as inclusions in a porphyroblastic cordierite matrix, and in sapphirine + K-feldspar symplectite in the vicinity of cordierite grains. In a second habit, sapphirine is symplectically intergrown with K-feldspar or plagioclase, occurring as radiating sheaves or rosettes without any preferred orientation. The sapphirine + plagioclase symplectites seem to replace sillimanite

porphyroblasts. The sapphirine + K-feldspar symplectites occur near biotite-rich layers and seem to replace cordierite porphyroblasts. These sapphirine + K-feldspar intergrowths contain biotite grains.

Modally, biotite constitutes 25% of the thin sections. It occurs as tiny (10 μm) platy inclusions in cordierite porphyroblasts, in symplectitic sapphirine, and in plagioclase (Fig. 3). Locally, biotite occurs as anhedral platy grains (≤ 0.5 cm) in the biotite-rich layers.

Plagioclase (15%) and K-feldspar (10%) have three habits (Fig. 3): 1) both can form subhedral porphyroblastic grains (≤ 0.5 cm) containing inclusions of biotite and cordierite, with typical polysynthetic twins and tartan twin domains, respectively. The K-feldspar contain exsolved blebs of sodic plagioclase, defining a

microperthitic texture. The platy plagioclase porphyroblasts are commonly partially replaced by white mica. 2) Plagioclase and K-feldspar occur as inclusions in spinel and in sapphirine. 3) Both plagioclase and K-feldspar occur in a symplectitic intergrowth with sapphirine, either as platy lamellae or as small polygonal crystals. K-feldspar also occurs as a corona around sapphirine.

Cordierite (15%) occurs as anhedral porphyroblasts (0.5 cm), some with typical twins, others containing zircon inclusions with pleochroic haloes (Fig. 3). Small inclusions of biotite are common. Cordierite also occurs as inclusions in porphyroblastic plagioclase, or as tiny grains between sapphirine lamellae associated with plagioclase.

Sillimanite (7%) has two habits (Fig. 3). It forms large (1 cm), birefringent, anhedral grains (Sil-1) corroded by sapphirine + plagioclase symplectites. This sillimanite contains plagioclase inclusions. A second generation of sillimanite (Sil-2) occurs as needles (0.2 cm) at the edge of the sillimanite porphyroblasts. These needles appear to cross-cut the Sil-1 grains. This Sil-2 occurs in association with biotite, cordierite and plagioclase.

clase, and in the sapphirine + K-feldspar symplectitic intergrowth.

Spinel (3%) is surrounded by a sapphirine or feldspar corona, or by sapphirine + K-feldspar symplectite (Fig. 3). Where it is in contact with cordierite porphyroblasts, it is surrounded by a sapphirine corona. Spinel in contact with biotite shows a cordierite corona. Corundum is present.

On the micrometer scale, spinel is partly replaced by corundum + hematite (Fig. 3). In this state, spinel is surrounded by a sapphirine corona. Where quartz is present, the spinel is surrounded by a cordierite or by a sapphirine corona. Locally, corundum forms small grains ($\leq 200 \mu\text{m}$) replacing spinel.

MINERAL COMPOSITIONS

Analytical method

Representative compositions of sapphirine, biotite, cordierite, K-feldspar, plagioclase and spinel (Tables 1 to 5) were obtained with the McGill University JEOL 8900 microprobe. We used five wavelength-dispersion spectrometers (WDS), a Si(Li) energy-dispersion (EDS) detector for semiquantitative analyses, secondary and back-scattered electron imaging, with magnification from 40 to 300,000 \times and 70 nm resolution, and high-resolution digital X-ray mapping by both EDS and WDS spectrometers and image-processing software for image analysis. Minerals were routinely analyzed for Na, Mg, Al, Si, K, Ca, Ti, Mn, Cr, Zn and Fe; biotite was also analyzed for F and Cl. Over 225 mineral analyses have been complemented by back-scattered electron imagery to define the spatial and textural compositional relationships described below.

Mineral compositions

The sapphirine shows minor variability in X_{Mg} (Table 1). The symplectitic sapphirine is generally slightly more magnesian (X_{Mg} 0.77, on average) than the sapphirine rimming hercynite (X_{Mg} 0.76, on average). This range of values is similar to that reported for metapelites in Enderby Land and in the Rauer Group (Harley 1986, 1998), but is higher than reported for sapphirine-bearing xenoliths from the Popes Harbour dyke in Nova Scotia, Canada (Owen & Greenough 1991). The sapphirine has a variable $X_{\text{Fe}^{3+}}$ (0.15–0.23, recalculated from stoichiometry, Table 1), and has only traces of Cr ($< 0.04 \text{ wt}\% \text{ Cr}_2\text{O}_3$).

The biotite has relatively high magnesium content ($\leq 17 \text{ wt}\%$, Table 2), and is thus phlogopite. Biotite inclusions in cordierite porphyroblasts have lower Ti (2–2.8 wt% TiO_2) than biotite inclusions in porphyroblastic plagioclase ($3.35 < \text{TiO}_2 < 3.65 \text{ wt}\%$, Table 2).

K-feldspar and plagioclase vary in Na content according to their textural context (Fig. 4, Table 3). The plagioclase in inclusions in sapphirine is more sodic

TABLE 1. REPRESENTATIVE COMPOSITIONS OF SAPPHIRINE FROM THE DOUGLAS HARBOUR DOMAIN, QUEBEC

Sample*	Spr1 3-c2a 3c rim	Spr2 3-c3a 3d rim	Spr3 8-c2 3l Pl symp	Spr4 13-c3a 3j Kfs symp	Spr5 7-c1 3j-3r Kfs symp	Spr6 16-c1 3f Pl symp
SiO ₂ wt.%	11.62	11.96	11.43	11.77	11.70	11.48
TiO ₂	0.05	0.03	0.01	0.03	0.01	0.01
Al ₂ O ₃	64.32	63.70	64.72	64.49	64.51	65.07
Cr ₂ O ₃	0.00	0.00	0.00	0.01	0.00	0.01
FeO	8.50	8.84	8.32	8.52	8.45	8.12
MnO	0.17	0.19	0.20	0.17	0.15	0.14
MgO	15.25	15.30	15.25	15.02	15.08	15.30
ZnO	0.03	0.00	0.00	0.00	0.00	0.00
Total	99.94	100.02	99.93	100.01	99.90	100.13
Si <i>apfu</i>	1.39	1.43	1.37	1.41	1.40	1.37
IV Al	4.61	4.57	4.63	4.59	4.60	4.63
Sum	6.00	6.00	6.00	6.00	6.00	6.00
VI Al	4.47	4.42	4.50	4.50	4.50	4.51
Ti	-	-	-	-	-	-
Fe ³⁺ ***	0.18	0.19	0.19	0.13	0.14	0.17
Mg	2.72	2.73	2.72	2.68	2.69	2.72
Fe ²⁺ ***	0.66	0.69	0.63	0.72	0.70	0.64
Mn	0.02	0.02	0.02	0.02	0.01	0.01
Cr	-	-	-	-	-	-
Zn	-	-	-	-	-	-
Sum	8.05	8.05	8.06	8.05	8.04	8.05
Fe	0.85	0.88	0.83	0.85	0.84	0.81
X_{Mg} **	0.76	0.76	0.77	0.76	0.76	0.77
$X_{\text{Fe}^{3+}}$ ***	0.80	0.80	0.81	0.79	0.79	0.81
$X_{\text{Fe}^{2+}}$ ***	0.21	0.21	0.23	0.15	0.17	0.21
$X_{\text{Fe}^{3+}}$ ***	23.6	24.4	23.2	24.1	23.8	22.9

(*) 3-c2a: Spr in a circular corona in Crd matrix; 3-c3a: Spr in circular corona within a Spr + Kfs symplectite (symp for short); 8-c2: Spr in a Spr + Pl symplectite replacing Sil; 13-c3a: Spr in a Spr + Kfs symplectite near a Crd porphyroblast; 7-c1: Spr in a Spr + Kfs symplectite; 16-c1: Spr in a Spr + Pl symplectite. See Table 5 for Spl composition. (**): $X_{\text{Mg}} = \text{Mg}/(\text{Mg} + \text{Fe})$; (***) $X_{\text{Fe}^{3+}} = \text{Fe}^{3+}/(\text{Fe}^{2+} + \text{Fe}^{3+})$, $X_{\text{Fe}^{2+}} = \text{Fe}^{2+}/(\text{Fe}^{2+} + \text{Fe}^{3+})$, and $\text{Fe} = 100(\text{Fe}^{2+} + \text{Fe}^{3+})/(\text{Fe}^{2+} + \text{Fe}^{3+} + \text{Mg})$. Compositions have been recalculated on the basis of 20 atoms of oxygen per formula unit (apfu): (Mg, Fe³⁺, Fe²⁺, Al)₈(Al, Si)₈O₁₈, after Deer *et al.* (1994).

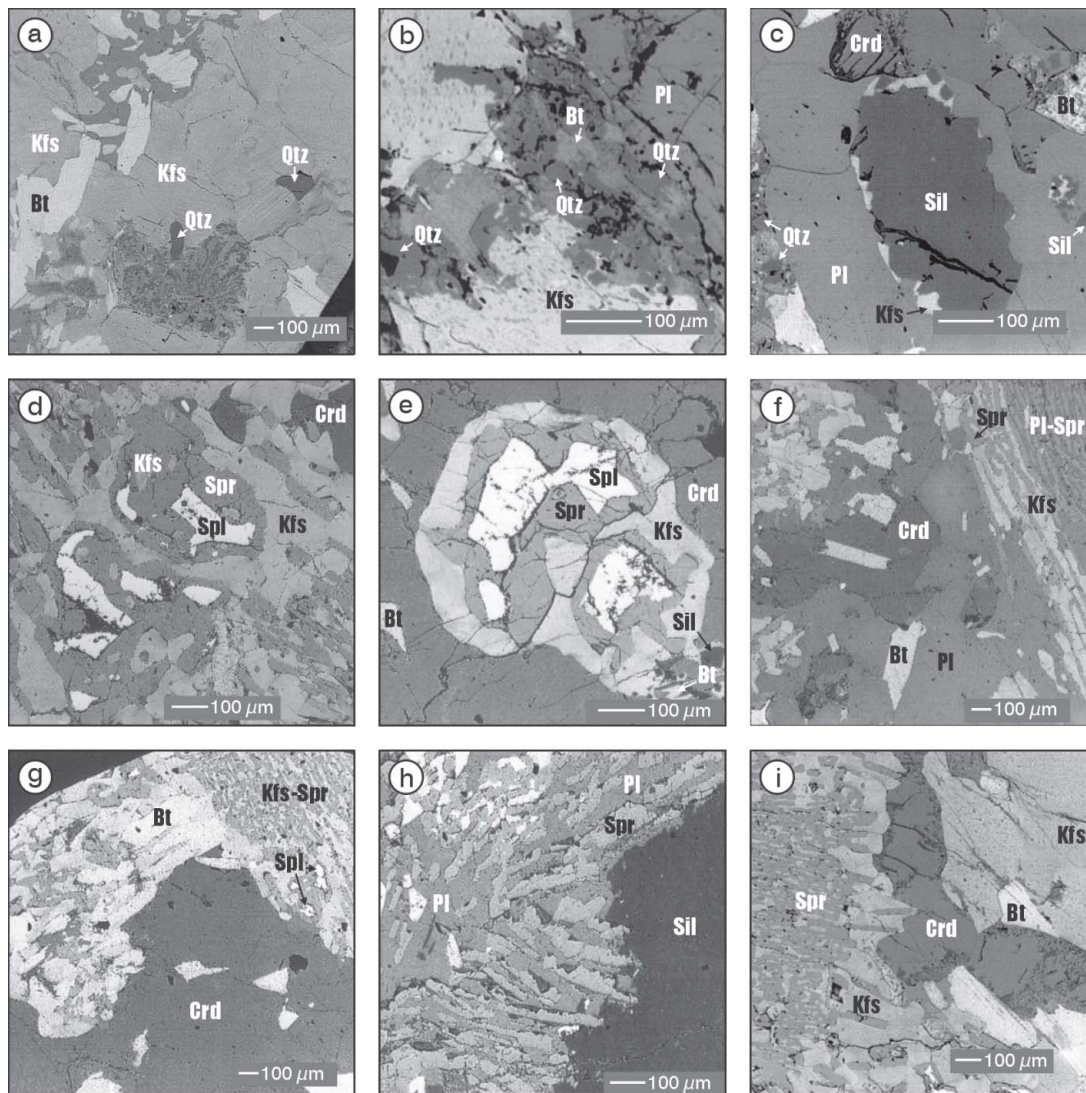
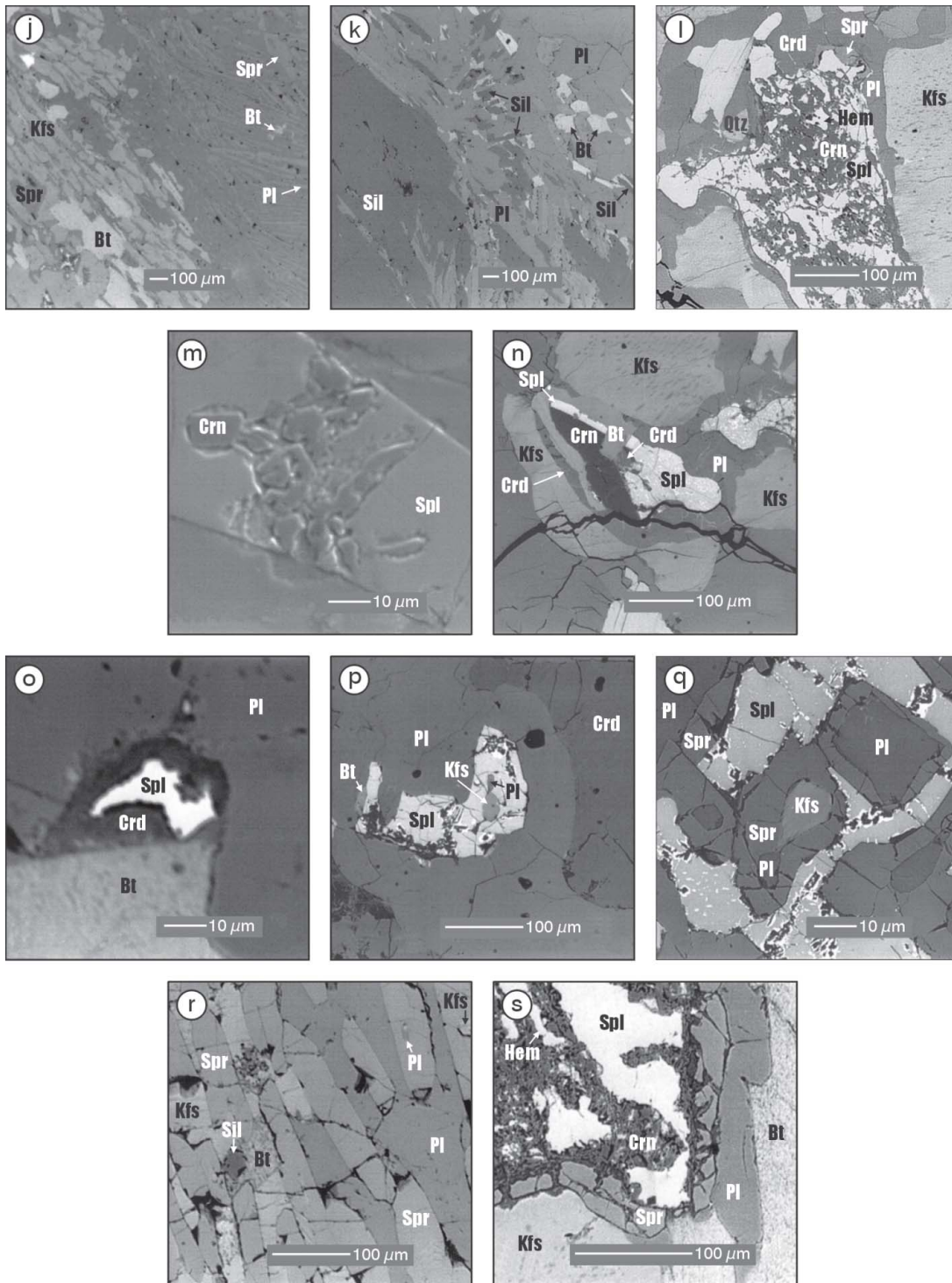


FIG. 3. Microphotographs of textures in the sapphirine-bearing xenolith from the Troie Complex. Minerals abbreviations according to Kretz (1983). (a, b, c). Anhedral microcrystalline Qtz. Bt, Kfs and Sil are present. (d) Subcircular corona of Spr around Spl + Kfs. This texture is found within the Spr + Kfs symplectites. (e) Circular corona with Spr surrounding Spl, and itself rimmed by Kfs. These textures are found in the cordierite-porphyroblast-bearing matrix. Note the Sil and Bt (left bottom) in Crd the porphyroblast. (f) Porphyroblastic Crd in PI porphyroblast, with adjacent Spr + Kfs or PI (or both) symplectitic textures. (g) Porphyroblastic Crd enclosed in a Spr + Kfs symplectitic texture with Bt inclusions. (h) Sil porphyroblast replaced by Spr + PI symplectitic texture. Note the presence of Bt in the Spr + Kfs symplectites. (i) Crd + Bt replaced by Spr + Kfs symplectitic textures. (j) Spr + Kfs or PI (or both) in a symplectitic texture. Note the presence of Bt in the Spr + Kfs symplectites. (k) Two generations of Sil: large porphyroblastic grain with PI inclusions (left) and small subhedral grains (right). (l) Destabilization of Spl = Crn + Hem. Qtz in contact with Spl rimmed by Crd or Spr (or both). (m) Crn inclusions replacing Spl. (n) Crn grain replacing Spl. Crd, Kfs and PI rim the Spl. (o) Bt + Spl = Crd reaction. (p) PI and Kfs inclusions in Spl rimmed by PI. (q) PI and Kfs inclusions in Spl rimmed by Spr. (r) Spr + Kfs or PI (or both) in a symplectitic texture. PI and Kfs in inclusions in Spr. Bt relics in Spr + Kfs symplectites. Sil is present. (s) Destabilization of Spl in Crn + Hem. Spl is rimmed by Spr.



(An₂₆) than plagioclase in spinel, or in sapphirine symplectite (An₃₆). Individual porphyroblasts of plagioclase are the least sodic (An₄₀). The K-feldspar is most sodic (Or₇₃Ab₂₇) in spinel inclusions, whereas grains found included in sapphirine or in symplectitic intergrowth are more potassic (Or₈₇₋₈₅Ab₁₃₋₁₅).

The cordierite is magnesian ($X_{Mg} \leq 0.85$, Table 4) and has a rather uniform composition. The analytical totals are in the range 97.5 to 98.5% and suggest the presence of minor H₂O or CO₂. In the Troie Complex, the cordierite has a lower X_{Mg} than that in Enderby Land (0.87 < X_{Mg} < 0.90; Harley 1986) and in the Rauer Group ($X_{Mg} = 0.89 \pm 0.06$; Harley 1998).

The two generations of sillimanite show similar compositions and contain less than 0.5 wt% Fe₂O₃.

Members of the spinel-hercynite solid-solution series contain only minor amounts of Cr, Zn and Fe³⁺. Gahnite (ZnAl₂O₄) and galaxite (MnAl₂O₄) components constitute ~1%. Contents of Fe³⁺ calculated from stoichiometry yield $X_{Fe^{3+}}$ values in the range 0.03–0.17 (Table 5), representing ~5% magnetite component, similar to that associated with sapphirine analyzed by Owen & Greenough (1991). Values of X_{Mg} are similar to the hercynite from Enderby Land (Harley 1986) and the Rauer Group (Harley 1998). Grains enclosed by a sapphirine + K-feldspar corona in porphyroblastic cordierite are slightly more magnesian (0.49 < X_{Mg} < 0.54) than

hercynite grains enclosed by sapphirine + K-feldspar symplectites ($X_{Mg} \leq 0.49$, Table 5).

TABLE 3. REPRESENTATIVE COMPOSITION OF FELDSPARS FROM THE DOUGLAS HARBOUR DOMAIN, QUEBEC

Sample* Photo Type	Pl1 P18S7 3r in Spr	Pl2 8-c1 3l Spr symp	Pl3 P1S5 3r Spr symp	Pl4 1-c1 3f porphyro- blast	Kfs1 6-c2a 3q in Spl	Kfs2 4-c2a 3c corona	Kfs3 5-c1 3j Spr symp	Kfs4 P18S6 3r Spr symp
SiO ₂ wt. %	60.00	58.98	59.40	56.67	65.28	64.99	64.55	63.81
Al ₂ O ₃	25.31	26.08	25.78	27.67	19.13	18.98	18.70	18.77
FeO	0.37	0.03	0.50	0.03	0.09	0.16	0.06	0.51
CaO	5.17	7.79	7.17	9.63	0.29	0.13	0.14	0.15
Na ₂ O	8.20	7.03	7.47	6.14	3.61	2.89	2.15	2.10
K ₂ O	0.61	0.17	0.09	0.15	11.83	12.86	14.21	13.73
Total	99.66	100.08	100.41	100.29	100.23	100.01	99.81	99.07
Si apfu	10.73	10.52	10.57	10.15	11.88	11.90	11.91	11.86
Al	5.33	5.48	5.41	5.84	4.10	4.09	4.06	4.11
Sum	16.06	16.00	15.98	15.99	15.98	15.99	15.97	15.97
Ca	0.99	1.49	1.37	1.85	0.06	0.03	0.03	0.03
Na	2.84	2.43	2.58	2.13	1.27	1.01	0.77	0.76
K	0.14	0.04	0.02	0.03	2.75	3.00	3.34	3.25
Sum	3.97	3.96	3.97	4.01	4.08	4.06	4.14	4.04
Fe	0.06	-	0.07	-	0.01	0.02	0.01	0.08
Ab**	71.56	61.42	65.01	53.11	31.24	25.30	18.57	18.72
An**	24.93	37.61	34.48	46.03	1.39	0.63	0.67	0.74
Or**	3.50	0.98	0.52	0.85	67.37	74.07	80.76	80.54

(*): P18S7: Pl in Spr; 8-c1: Pl in Spr + Pl symplectite; P1S5: Pl in Spr + Pl symplectite; 1-c1: porphyroblastic Pl; 6-c2a: Kfs in spinel; 4-c2a: Kfs in circular corona; 5-c1: Kfs in a Spr + Kfs symplectite; P18S6: Kfs in Spr. (**): Kfs and Pl: Ab = 100Na/(Ca + Na + K), An = 100Ca/(Ca + Na + K), Or = 100K/(Ca + Na + K). Structural formulae normalized to 32 atoms of oxygen.

TABLE 2. REPRESENTATIVE COMPOSITIONS OF BIOTITE FROM THE DOUGLAS HARBOUR DOMAIN, QUEBEC

Sample [†] Photo	Bt1 5-c3 3g	Bt2 8-c3 3j	Bt3 5-c1 3f
SiO ₂ wt. %	36.75	36.16	35.76
TiO ₂	2.78	2.84	3.38
Al ₂ O ₃	18.86	18.69	18.85
FeO	10.10	9.56	9.62
MgO	16.87	16.25	15.94
CaO	0.02	0.07	0.04
K ₂ O	10.56	10.34	10.47
Na ₂ O	0.17	0.20	0.11
MnO	0.05	0.05	0.05
Cr ₂ O ₃	0.01	0.01	0.00
Total	96.17	94.17	94.22
Si apfu	5.19	5.21	5.17
Al	2.81	2.79	2.83
Sum	8.00	8.00	8.00
Al	0.33	0.39	0.38
Ti	0.29	0.31	0.37
Fe	1.19	1.15	1.16
Mn	-	0.01	-
Mg	3.55	3.49	3.44
Cr	-	-	-
Sum	5.07	5.35	5.35
Ca	-	0.01	-
K	1.90	1.90	1.93
Na	0.05	0.05	0.03
Sum	1.95	1.96	1.96
X_{Mg}^{**}	0.75	0.75	0.75

([†]): 5-c3: Bt in porphyroblastic Crd; 8-c3: Bt in Spr + Kfs symplectite; 5-c1: Bt in porphyroblastic Pl. (**): $X_{Mg} = Mg/(Mg + Fe)$. The structural formulae are normalized to 22 atoms of oxygen per formula unit (apfu), ignoring H₂O, F, Cl. In all three cases, the biotite is phlogopite.

TABLE 4. REPRESENTATIVE COMPOSITION OF CORDIERITE FROM THE DOUGLAS HARBOUR DOMAIN, QUEBEC

Sample [†] Photo Type	Crd1 6-c3 3g core	Crd2 6-c3 3g rim	Crd3 5-c2a 3c corona	Crd4 2-c1 3f in Pl
SiO ₂ wt. %	49.08	49.37	49.17	48.60
TiO ₂	0.00	0.02	0.00	0.01
Al ₂ O ₃	34.07	34.32	34.24	34.28
Cr ₂ O ₃	0.00	0.00	0.00	0.01
FeO	3.52	3.46	3.46	3.52
MnO	0.09	0.13	0.11	0.11
MgO	11.26	11.37	11.36	11.38
Na ₂ O	0.15	0.11	0.11	0.09
CaO	0.03	0.00	0.00	0.00
Total	98.20	98.78	98.45	98.00
Si apfu	4.95	4.95	4.95	4.92
Al	1.05	1.05	1.05	1.08
Sum	6.00	6.00	6.00	6.00
Al	3.00	3.00	3.01	3.01
Fe ²⁺	-	-	-	-
Cr	-	-	-	-
Mg	1.69	1.70	1.70	1.71
Mn	-	0.01	0.01	0.01
Fe ³⁺	0.30	0.29	0.29	0.30
Sum	1.99	2.00	2.00	2.01
Na	0.03	0.02	0.02	0.02
Ca	-	-	-	-
X_{Mg}^{**}	0.85	0.85	0.85	0.85

([†]): 6-c3: porphyroblastic Crd near Spr + Kfs symplectite; 5-c2a: porphyroblastic Crd around the Spl + Spr + Kfs circular corona texture; 12-c1: Crd in porphyroblastic Pl. (**): $X_{Mg} = Mg/(Mg + Fe)$. Structural formulae normalized to 18 atoms of oxygen.

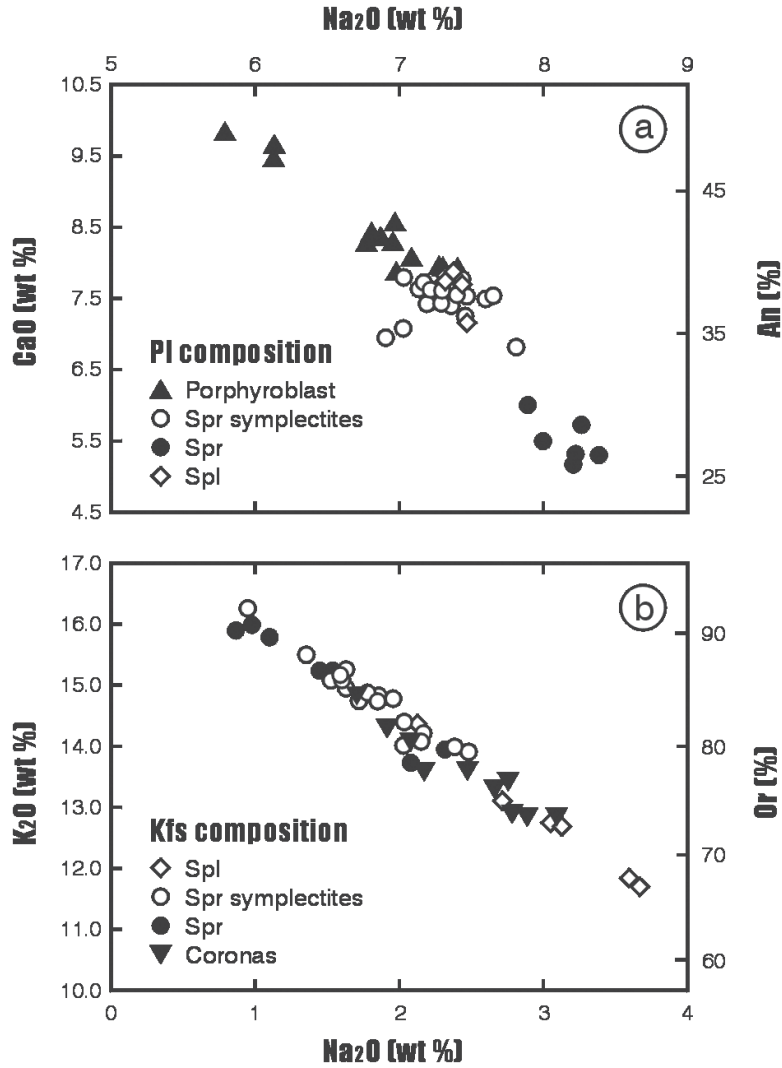


FIG. 4. Compositions of plagioclase and K-feldspar depending of their textural associations.

INTERPRETATION OF TEXTURES

A wide variety of reaction textures are developed in thin section, suggesting a multistage or highly localized evolution. The assemblages and textures are similar to those described by Harley (1986, 1998) in Enderby Land, Antarctica and in the Rauer Group by Nijland *et al.* (1998) in southern Norway. Many of the sapphirine occurrences documented in the literature indicate the presence of garnet and orthopyroxene in the assemblages. In the sample studied here, garnet and orthopyroxene are absent. Considering the reactants and products strictly within the system FMASH (or MASH,

regarding $\text{FeO} = \text{MgO}$, and assuming some minor replacement of Al by Fe^{3+}), textures indicate an early spinel-bearing assemblage that was succeeded by a sapphirine–cordierite-bearing assemblage.

Early assemblage of minerals

Many sapphirine grains contain inclusions of relict hercynite (Fig. 3). In turn, the hercynite contains relics of K-feldspar and plagioclase (Fig. 3). This occurrence suggests an early hercynite-bearing assemblage, in which hercynite coexisted with sillimanite, biotite, feldspar and quartz; this assemblage then reacted to form

cordierite, sapphirine and a second generation of feldspar and sillimanite. The replacement of hercynite by sapphirine and cordierite could be accomplished by reactions with added silica. The regional geology shows that the sapphirine xenolith is found in an enderbite intrusion (TC, Fig. 2). The silica seems to be introduced from a silica-rich environment into a silica-poor environment, which was invaded from the matrix by quartz veins. In this case, the minerals that mantle and armor each other may be the result of reaction among pre-existing stable assemblages. This mode of origin explains most sapphirine-bearing assemblages (Herd 1991).

Appearance of cordierite and sapphirine

Several combinations and permutations of the minerals described above can be combined to account for

the second generation of metamorphic minerals (Table 6). The presence of K-feldspar and plagioclase intergrown with sapphirine may indicate that these minerals took part in reactions, or may be the matrix within which reactions in the FMASH system took place. The presence of the same phases before and after reactions may mean they are both reactants and products, or they were stable and present while other phases reacted. The spatially restricted occurrence of these second-generation assemblages implies that equilibration was only local, even at the thin-section scale, and thus indicates mosaic equilibrium and global disequilibrium at the outcrop scale. As a result, certain minerals, sillimanite and feldspar for example, occur as both a reactant and a product depending upon the local reaction-volumes.

The formation of cordierite, corundum and feldspar

In thin section (Fig. 3), quartz is observed in contact with biotite and feldspar. Sillimanite and cordierite are locally present. Biotite occurs as inclusions in cordierite and feldspar along with sillimanite and quartz, suggesting a reaction of biotite to cordierite according to reactions (1) and (2) in Table 6. The occurrence of hercynite in contact with cordierite, biotite and K-feldspar, cordierite in a corona around hercynite, and quartz in contact with cordierite around hercynite, all suggest the formation of cordierite from hercynite *via* reactions (3), (4) and (5) in Table 6. The variable composition and habit of feldspar, both as inclusions in hercynite and as coronas around hercynite, suggest that it may serve as both a reactant and a product of hercynite breakdown (reaction (6)). Corundum found intimately associated with hercynite may represent a residual product of the breakdown of hercynite (reaction (7)). Corundum is currently observed in contact with cordierite and K-feldspar. Hercynite and biotite are altered. Cordierite forms by the breakdown of hercynite, sillimanite and biotite *via* reactions (8) and (9), where corundum is a residual product.

The formation of sapphirine

Quartz, an essential reactant, is progressively consumed in reactions (1), (2) and (5) (Table 6). There is no evidence for Spl + Qtz pre-existing in contact, although hercynite is texturally an early phase. This finding argues for hercynite in a silica-poor matrix prior to reaction with quartz, which would mean that the quartz had been introduced. In areas deficient in quartz, hercynite and biotite, along with cordierite and feldspar, give rise to sapphirine – K-feldspar symplectites *via* reactions (11), (12) and (13) in Table 6.

Sillimanite porphyroblasts contain plagioclase inclusions and are surrounded by symplectites of Spr + Pl. Plagioclase and cordierite can be regarded as interchangeable in terms of their Al : Si ratios, and also in terms of the roles they play in a reaction (Harley 1998),

TABLE 5. REPRESENTATIVE COMPOSITION OF HERCYNITE FROM THE DOUGLAS HARBOUR DOMAIN, QUEBEC

Sample ¹ Photo Type	He1 10-c2a 3c corona	He2 4-c3a 3d corona		He1 10-c2a	He2 4-c3a
SiO ₂ wt. %	0.00	0.00	Si <i>apfu</i>	-	-
TiO ₂	0.00	0.01	Ti	-	-
Al ₂ O ₃	63.07	62.99	Al	15.70	15.68
Cr ₂ O ₃	0.05	0.00	Cr	-	-
FeO	24.70	25.53	Fe ^{2+***}	0.39	0.41
MnO	0.30	0.24	<i>Sum</i>	16.09	16.09
MgO	12.71	12.34	Fe ^{2+***}	3.94	4.06
ZnO	0.17	0.21	Mn	0.05	0.04
Total	101.00	101.32	Mg	4.00	3.88
			Zn	0.03	0.03
			<i>Sum</i>	8.02	8.01
			X _{Fe²⁺} ^{***}	0.50	0.49
			X _{Fe³⁺} ^{***}	0.09	0.09

(¹): 10-c2a: Spl in corona in Crd porphyroblastic matrix; 4-c3a: He in corona in a Spr + Kfs symplectite. (**): Fe²⁺, Fe³⁺, X_{Mg}, X_{Fe³⁺} recalculated from stoichiometry with X_{Mg} = Mg/(Mg + Fe²⁺) and X_{Fe³⁺} = Fe³⁺/(Fe²⁺ + Fe³⁺). Structural formulae normalized to 32 atoms of oxygen.}

TABLE 6. LOCAL EQUILIBRIA REACTIONS RELATED TO THE TEXTURES OBSERVED IN FIGURE 3

Cordierite, corundum and feldspar formation	
Bt + Qtz = Sil + Kfs + Crd	(1)
Bt + Qtz + Sil = Kfs + Crd + H ₂ O	(2)
Spl + Bt = Crd + Kfs	(3)
Bt + Spl = Crd + Kfs	(4)
Spl + Qtz = Crd	(5)
Spl + Sil = Crn + Crd	(8)
Bt + Sil = Crn + Crd + Kfs + H ₂ O	(9)
Feldspar and corundum formation	
Spl + Pl + Kfs = Pl + Bt	(6)
Spl = Crn + Hem	(7)
Sapphirine formation	
Spl + Crd = Spr	(10)
Spl + Crd + Bt = Spr + Kfs	(11)
Spl + Pl (Kfs) = Spr + Pl (Kfs)	(12)
Spl + Pl = Spr + Crn + Pl	(13)
Spl + Sil = Spr + Crn	(14)

which may explain the presence of plagioclase rather than cordierite in the sapphirine + plagioclase symplectites (reaction (12)).

Sapphirine surrounding hercynite also may originate through reactions (11) and (12). The fact that remnant spinel contains appreciable hercynite component as well as corundum and hematite inclusions supports the hypothesis of Podlesskii & Kurdyukov (1992), who suggested that sapphirine may in some cases develop by a retrograde reaction at the expense of the magnesian component of spinel. The formation of corundum by reaction (8) implies two further sapphirine-forming reactions, at the expense of hercynite surrounded by sapphirine and cordierite; corundum may have been produced by reactions (13) and (14).

The localized occurrence of these textures indicates a mosaic equilibrium whose progress was arrested owing to limited migration of elements. The implication of introduction of silica, K-feldspar, plagioclase and H₂O implies that the assemblages arose by introduction of "granitic" material into a silica-poor protholith. This is a common origin for sapphirine-bearing rocks in many localities (Herd 1991). If the process is arrested, the sapphirine-bearing assemblages are preserved. If not, eventually sapphirine, spinel and other refractory phases may be converted to an assemblage containing cordierite, sillimanite, ± corundum, biotite, quartz and feldspar, for example. Because of introduced material, it may appear that there is disequilibrium throughout the rock. In fact, there may essentially be equilibrium in each part of the rock, but different assemblages because of different bulk-compositions owing to concentration gradients. We infer that the absence of garnet and orthopyroxene, more representative of this facies, is due to the highly aluminous bulk-composition of the rock and its relatively low content in iron.

THERMOBAROMETRY

Because of a lack of thermochemical data for Fe-rich sapphirine, and differences in composition between natural and synthetic sapphirine (Owen & Greenough 1991), the P–T conditions of its formation are commonly based on the composition of associated solid-solutions. In this study, temperatures were calculated using thermometers based on Fe–Mg exchanges between sapphirine and spinel (Owen & Greenough 1991), spinel and cordierite (Vielzeuf 1983), and the TWEEQU software (Berman 1991). Pressure estimates are handicapped by the absence of pressure-indicator phases, such as garnet. However, the presence of quartz, spinel, cordierite, sillimanite and corundum allows us to use the assemblages Spl – Crd – Qtz and Sil – Spl – Crn – Crd as geothermobarometers with the database of Berman (1991). Each reaction and each assemblage needed to determine P–T conditions are based on interpretation of textures in each zone observed at the thin-section scale.

The sapphirine–spinel geothermometer

Owen & Greenough (1991) proposed an empirical geothermometer based on Fe–Mg exchange between spinel and sapphirine with $X_{Mg} < 0.9$ and $X_{Fe^{3+}} < 0.4$. Use of this thermometer is probably appropriate for the sample studied here, since the spinel is poor in the garnite component, and sapphirine has a value of X_{Mg} in the range 0.71–0.85, and of $X_{Fe^{3+}}$ in the range 0.15–0.23. Coronas with a spinel core yield temperatures of 815–920 ± 100°C (Table 7). Temperatures calculated using compositions of the spinel cores are the highest (>900 ± 100°C). The corona developed within the symplectites yield temperatures of 820–860 ± 100°C, with a maximum using core compositions of spinel (Table 7). In contrast, sapphirine + K-feldspar and sapphirine + plagioclase symplectites yield lower temperatures (755–845 and 780–875 ± 100°C, respectively).

The cordierite–spinel geothermometer

Vielzeuf (1983) proposed a geothermometer based on Fe–Mg exchange between spinel and cordierite (hercynite + cordierite = spinel + sekaninaite). Porphyroblastic cordierite in this rock (Fig. 3g) yields a high temperature (960–1070°C), with no difference between the core and the rim of grains (Table 8). Cordierite included in porphyroblastic plagioclase (Fig. 3f) yields similar temperatures (890–1160°C). These temperatures are significantly higher than those derived from the spinel–sapphirine geothermometer.

TABLE 7. CALCULATION OF TEMPERATURE CONDITIONS USING THE SAPPHIRINE–SPINEL THERMOMETER

Sample ^(*)	Photo	Spr X_{Mg} ^(**)	Spl X_{Mg} ^(***)	$\ln K_j$ ^(*)	T ^(*) ±100°C
3251-c2a	3e	0.81	0.54	1.27	816
		0.80	0.50	1.38	842
		0.85	0.55	1.53	876
		0.85	0.50 (core)	1.73	921
3251-c3a	3e	0.79	0.51	1.28	819
		0.79	0.50	1.32	828
		0.79	0.49	1.36	837
		0.80	0.48 (core)	1.46	860
3251-c3ab	3d	0.77	0.55	1.01	757
		0.78	0.50	1.26	814
		0.77	0.48	1.29	821
		0.79	0.50	1.32	828
		0.79	0.48	1.40	846
3251-c1/c2	3d	0.79	0.55	1.12	782
		0.80	0.54	1.22	805
		0.79	0.50	1.32	828
		0.81	0.50	1.45	857
		0.81	0.48	1.53	876

(*) $K_j = (X_{Spr}/X_{Spl}) / (X_{Spr}/X_{Spl})$, and $T(^{\circ}C) = [800 + (228 \cdot \ln K_j) - 273] / X_{Mg}$ = $Mg/(Mg + Fe^{2+})$, recalculated from stoichiometry. (**): 3251-c2a: Spr–Spl in circular corona texture (Fig. 3c); 3251-c3a: Spr–Spl subcircular texture; 3251-c3ab: Spr–Spl with Spr in a Spr + Kfs symplectitic texture; 3251-c1/c2: Spr–Spl with Spr in a Spr + Pl symplectitic texture. (***) X_{Mg} recalculated from stoichiometry, with $X_{Mg} = Mg/(Mg + Fe^{2+})$. (****): $X_{Mg} = Mg/(Mg + Fe)$. The geothermometer used was proposed by Owen & Greenough (1991).

Geothermobarometers calculated using TWEEQU

Temperature and pressure estimates were also obtained using Berman's (1988, 1991) TWEEQU software (version 2.02), incorporating his internally consistent database BA96a. Generally, a maximum "aggregate uncertainty" of ± 1 kbar and $\pm 50^\circ\text{C}$ is adopted in calculations, based on the suggestions of Essene (1989) for conventional thermobarometry. One of the advantages of the TWEEQU technique is that the state of equilibration of the sample can be assessed by comparing the positions of intersection of all independent equilibria for a given assemblage. A good convergence is consistent with an inference of equilibrium, whereas divergence suggests that one or more phases were not in equilibrium with neighboring phases. The P-T calculations followed the method of Berman (1988, 1991). Activity-composition relations for biotite, cordierite, spinel and plagioclase were computed using the models of Berman (1988, 1991), Fuhrman & Lindsley (1988), Berman & Aranovitch (1996), Aranovitch & Berman (1996) and Berman *et al.* (1995). Sillimanite and quartz were assumed to be pure.

Summary of P-T estimates

From the textures described above, idealized reactions are suggested in Table 6 [(2), (5), (8) and (9)] that permit P-T estimates (curves 1, 2, 3, 4 and 6, Fig. 5) using results of electron-microprobe analyses of coexisting minerals and TWEEQU. The somewhat dispersed intersections of the reaction curves outline an area of P-T space rather than a single P-T point for the conditions of metamorphism. This is possibly due in part to the mosaic equilibria described above, but may also be a reflection of re-equilibration during cooling. The reactions do suggest an approximate maximum temperature of $1260 \pm 50^\circ\text{C}$ (Fig. 5). Minimum temperatures, on the other hand, occur at $770 \pm 50^\circ\text{C}$ (Fig. 5), with an average temperature near $810 \pm 50^\circ\text{C}$.

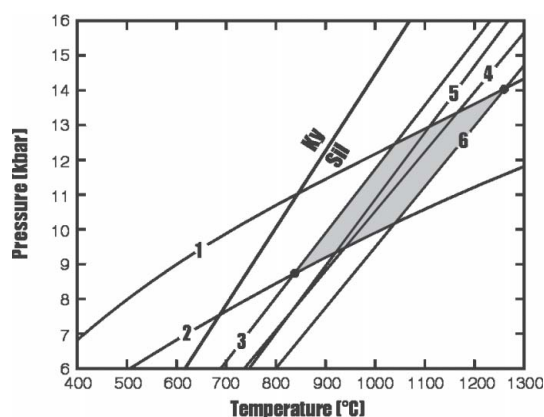
TABLE 8. CALCULATION OF TEMPERATURE CONDITIONS USING THE CORDIERITE-SPINEL THERMOMETER

Sample**	Crd	Spl-Hc	Ln K_d^*	T($^\circ\text{C}$) [†]
	X_{Mg}^{***}	X_{Mg}^{****}		
3251-c3	0.85	0.48	-1.81	958
	0.85	0.50	-1.73	1031
	0.85	0.51	-1.69	1070
3251-c1	0.86	0.48	-1.89	893
	0.86	0.49	-1.85	925
	0.86	0.51	-1.77	993
	0.86	0.54	-1.65	1113
	0.86	0.55	-1.61	1158

(*) $K_d = (X_{\text{SplMg}} * X_{\text{CrdFe}}) / (X_{\text{SplFe}} * X_{\text{CrdMg}})$, and T($^\circ\text{C}$) = $[-1763 / (\text{Ln}K_d + 0.378)] - 273$. (**): 3251-c3: porphyroblastic Crd (Fig. 3e); 3251-c1: Crd in porphyroblastic Pl (Fig. 3d). (***) $X_{Mg} = \text{Mg}/(\text{Mg} + \text{Fe})$; (****): X_{Spl} recalculated from stoichiometry with $X_{Mg} = \text{Mg}/(\text{Mg} + \text{Fe}^{2+})$. The geothermometer used was proposed by Vielzeuf (1983).

Pressure constraints place a maximum P near 14 ± 1 kbar and a minimum P near 7.5 ± 1 kbar (Fig. 5), with average pressures (calculated with different P-T results obtained by TWEEQU with the same thermobarometers as in Figure 5) near 13.3 ± 1 kbar and 8 ± 1 kbar, respectively. These pressures are at the high end of the range published for similar assemblages (Bertrand *et al.* 1991, Nichols *et al.* 1992, Harley 1998). Hensen (1987) located the FMAS [Qtz] invariant point at $920-950^\circ\text{C}$ and $8-9$ kbar from topological constraints and on the basis of natural assemblages; there are as yet no experimental determinations of the quartz-absent invariant point and related univariant lines (Harley 1998). Previous calculations using the garnet - orthopyroxene - biotite - plagioclase - quartz geobarometer for other metasedimentary relics in the Troie Complex have yielded P-T conditions between 9 and 11 ± 1 kbar and $800-950 \pm 50^\circ\text{C}$ (Goulet & Cadéron 2000). These results are in agreement with the conditions calculated here.

Estimates based on the Spl-Spr thermometer of Owen & Greenough (1991) indicate temperatures between 755 and $920 \pm 50^\circ\text{C}$. The Crd-Spl thermometer of Vielzeuf (1983) indicates temperatures between 890 and $1160 \pm 50^\circ\text{C}$. We estimate the P-T conditions of the Sil - Spl - Crd - Spr - Qtz assemblage studied here to be between 900 and $950 \pm 50^\circ\text{C}$ and $9-10 \pm 1$ kbar. It is probable that the existence of these sapphirine-bearing assemblages indicate temperatures of at least 800°C .



- 1: $2 \text{ Spl} + 5 \alpha\text{Qtz} = \text{Crd}$
- 2: $2 \text{ Spl} + 5 \text{ Sil} = 5 \text{ Crn} + \text{Crd}$
- 3: $2 \text{ Ann} + 9 \alpha\text{Qtz} + 6 \text{ Sil} = 2 \text{ Kfs} + 3 \text{ Skn} + 2 \text{ H}_2\text{O}$
- 4: $2 \text{ Phl} + 9 \alpha\text{Qtz} + 6 \text{ Sil} = 2 \text{ Kfs} + 3 \text{ Crd} + 2 \text{ H}_2\text{O}$
- 5: $2 \text{ Ann} + 15 \text{ Sil} = 9 \text{ Crn} + 3 \text{ Skn} + 2 \text{ Kfs} + 2 \text{ H}_2\text{O}$
- 6: $15 \text{ Sil} + 2 \text{ Phl} = 9 \text{ Crn} + 3 \text{ Crd} + 2 \text{ Kfs} + 2 \text{ H}_2\text{O}$

FIG. 5. TWEEQU P-T diagram showing calculations of reactions (2), (5), (8) and (9) illustrated in Table 6. These reactions correspond to curves respectively noted (3,4), (1), (2) and (5,6) in the Figure.

and 10 kbar (Herd 1991). Indeed, the photomicrographs (Fig. 3) suggest that some reaction textures (rims and symplectites) are preserved, and also a significant amount of annealing and polygonization, which obscures reaction textures, and suggests that at least some of the assemblages were held under static P–T conditions for a protracted period. This textural interpretation, together with the P–T conditions inferred, seem in good agreement with a protracted cooling event following a short-lived high-temperature pulse. This period could be related to the emplacement of the enderbite

intrusion of the Troie Complex (TC). This complex represents a large volume (Fig. 2) of a hot (810–1045°C) dry magma, leading to a long period of cooling under relatively static P–T conditions.

The P–T grid

Attempts to model the many reactions on a petrogenetic grid are hampered by the large number of components needed to define the compositional space of this assemblage and the large uncertainties or total lack of

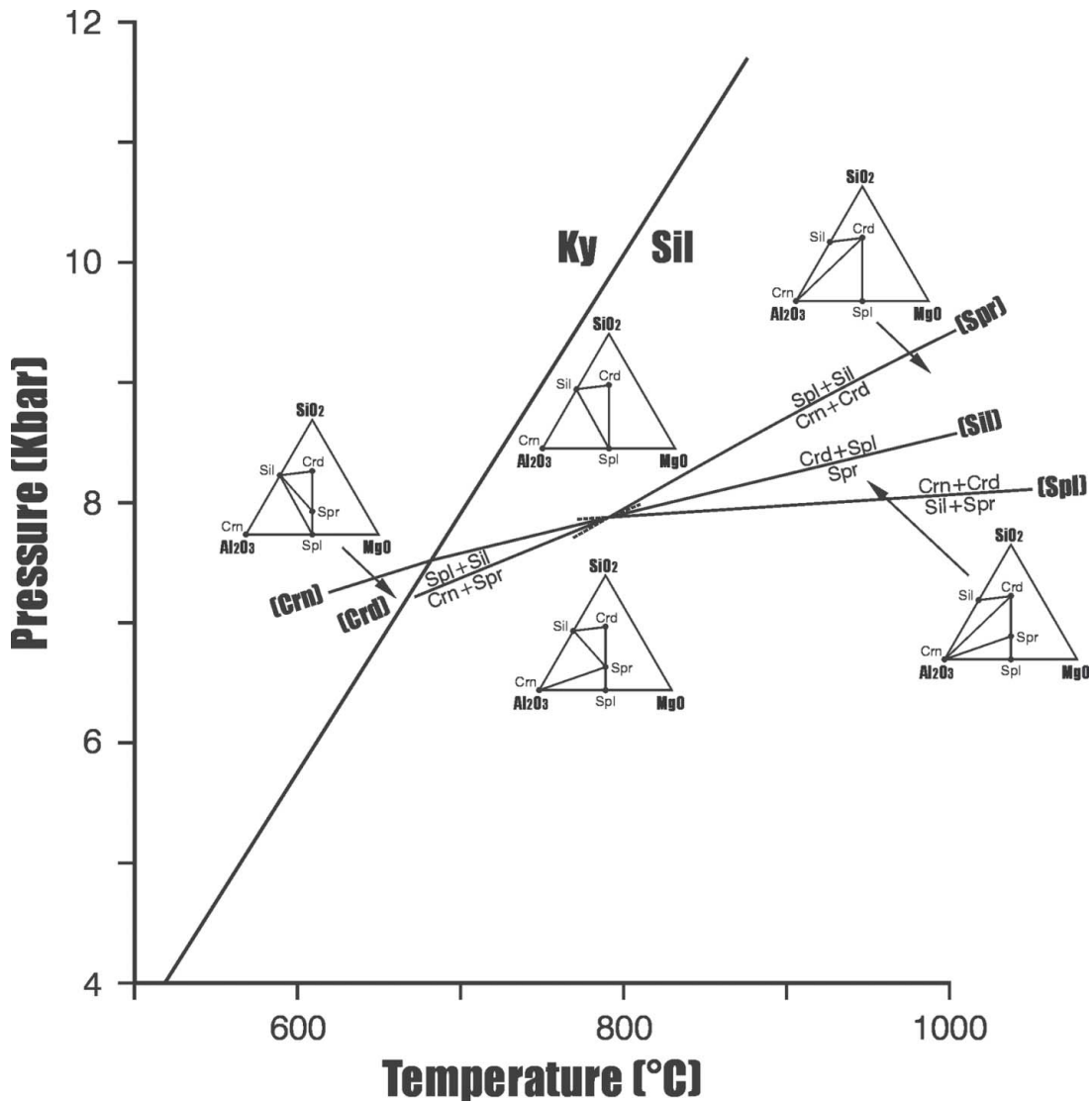


FIG. 6. P–T grid for Crn–Crd–Sil–Spr–Spl in the system MgO–Al₂O₃–SiO₂–H₂O (MASH system). The mineral symbols are those of Kretz (1983).

data that exist in the thermodynamic databases for several of the minerals in the assemblage. One can postulate a simplified grid (Fig. 6) in the ideal system MgO–Al₂O₃–SiO₂–H₂O (MASH), which includes the observed minerals corundum, sapphirine, cordierite, sillimanite and spinel. Quartz, which occurs in vanishingly small quantities, need not be considered.

The kyanite-to-sillimanite transition and the (Spr) reaction (Fig. 6) are correctly situated relative to P and T using TWEEQU. The slope of the (Crd) reaction is only slightly more positive than that of the (Spr) reaction, given that both reactions involve spinel plus sillimanite as reactants. The (Crn) and (Sil) reactions involve the same minerals and are colinear with the univariant line, refracting across the kyanite to sillimanite transition. The positive slopes of the colinear and (Spl) reactions are here constrained by considerations of the change of entropy and volume. Finally, the invariant point can slide up and down any of the univariant lines, but must stay in the sillimanite field. The grid as presented thus demonstrates that sapphirine is a product of several different reactions, and that sillimanite can be either a reactant or a product of reaction, interpretations that are consistent with petrographic observations. Although the invariant point is only constrained by the presence of sillimanite, the grid's stability does require a high temperature and pressure, supporting the other geothermobarometric calculations previously discussed.

DISCUSSION: THE TECTONIC MODEL

The mineralogical assemblage recorded in the xenolith we have studied suggests pressure conditions somewhere between 7.5 and 14 kbar (24–46 km). If the higher pressure obtains, then this greatly extends the range of pressure conditions inferred from other barometers for the Minto (maximum 8.4 kbar: Percival & Skulski 2000, Bédard 2003). Either the early history of cratonization in the northern Superior Province is marked by significant thickening of the crust, as advocated by Percival *et al.* (1992, 1994, 2001), or some mechanism existed to allow fragments of supracrustal rocks to founder to such depths and then rise again, perhaps through partial convective overturn (referred to as “sagduction” by others), as suggested by Collins *et al.* (1998) and Bédard *et al.* (2003).

In terms of supracrustal rocks, the transition from the Troie to the Faribault–Thury Complex corresponds to a change from granulite to amphibolite facies. Bédard (2003) proposed that metamorphism of the supracrustal belts is not due to an overprinting orogenic event as thought previously (Percival *et al.* 1992, 1994, Percival & Skulski 2000), but rather reflects advective transport of heat by the dominant felsic plutonic component of the crust. In this context, the peak conditions of temperature recorded in the xenolith we have described could plausibly reflect the massive influx of heat required to generate the enderbite magmas of the Troie

Complex. We speculate that the protracted period of static P–T conditions could reflect transport and ascent of the clast in an enderbite magma flowing upward advectively before a protracted retrograde event related to the cooling of the intrusion. Furthermore, the presence of symplectites involving sapphirine + K-feldspar or plagioclase (or both) is considered typical of decompressional textures (Spear 1993, Harley 1998), and would also imply an origin during a short-lived heating event coupled with rapid ascent, protracted period of cooling, and decompression of a large clast-charged enderbite intrusion.

ACKNOWLEDGEMENTS

Fieldwork in the 1998 and 1999 field seasons was supported by Géologie Québec, Ministère des Ressources Naturelles du Québec, contribution #2001–5130–21. We thank Louis Madore, who provided the sapphirine-bearing sample for study. An anonymous reviewer, Richard Herd, and Robert F. Martin provided major comments and precious corrections. We thank the FCAR for financial support. Glenn Poirier, formerly of the McGill Microprobe Laboratory, prepared the maps of compositional variation in the constituent minerals. Michèle Lanthier of the Université du Québec à Montréal drafted the figures. And to Dugald, thanks for introducing us to new ways at looking at metamorphic rocks via observation, mathematics and thermodynamics. Continue to intrigue us for many years to come! One of us (WT) is very happy to have been there from the beginning. To NG, Dugald was among the best teachers, and a true inspiration for his innovative and creative approach to geology.

REFERENCES

- ARANOVITCH, L.Y. & BERMAN, R.G. (1996): Optimized standard and mixing properties of minerals. II. Comparisons, predictions, and applications. *Contrib. Mineral. Petrol.* **126**, 25–37.
- ARIMA, M. & BARNETT, R. L. (1984): Sapphirine bearing granulites from the Sipiwek Lake area of the late Archean Pikwitonei Granulite terrain, Manitoba, Canada. *Contrib. Mineral. Petrol.* **88**, 102–112.
- AYRES, L. D. & THURSTON, P. C. (1985): Archean supracrustal sequences in the Canadian Shield – an overview. In *Evolution of Archean Supracrustal Sequences* (L.D. Ayres, P.C. Thurston, K.D. Card & W. Weber, eds.). *Geol. Assoc. Can., Spec. Pap.* **28**, 343–370.
- BÉDARD, J.H. (2003): Evidence for regional-scale, pluton driven, high-grade metamorphism in the Minto Block, northern Superior Province, Canada. *J. Geol.* **111**, 183–205.
- _____, BROUILLETTE, P., MADORE, L. & BERCLAZ, A. (2003): Archean cratonization and deformation in the northern Superior Province, Canada: an evaluation of plate

- tectonic vs vertical tectonic models. *Precamb. Res.* **127**, 61-87.
- BERMAN, R.G. (1988): Internally-consistent thermodynamic data for stoichiometric minerals in the system Na₂O–K₂O–CaO–MgO–FeO–Fe₂O₃–Al₂O₃–SiO₂–TiO₂–H₂O–CO₂. *J. Petrol.* **29**, 445-522.
- _____ (1991): Thermobarometry using multi-equilibrium calculations: a new technique with petrologic applications. *Can. Mineral.* **29**, 833-855.
- _____ & ARANOVICH, L.Y. (1996): Optimized standard state and mixing properties of minerals. I. Model calibration for olivine, orthopyroxene, cordierite, garnet, and ilmenite in the system FeO–MgO–CaO–Al₂O₃–TiO₂–SiO₂. *Contrib. Mineral. Petrol.* **126**, 1-24.
- _____, _____ & PATTISON, D.R.M. (1995): Reanalysis of the garnet–clinopyroxene Fe–Mg exchange thermometer. II. Thermodynamic analysis. *Contrib. Mineral. Petrol.* **119**, 30-42.
- BERTRAND, P., ELLIS, D.J. & GREEN, D.H. (1991): The stability of sapphirine–quartz and hypersthene – sillimanite – quartz assemblages: an experimental investigation in the system FeO–MgO–Al₂O₃–SiO₂ under H₂O and CO₂ conditions. *Contrib. Mineral. Petrol.* **108**, 55-71.
- COLLINS, W.J., KRANENDONK, M.J. & TEYSSIER, C. (1998): Partial convective overturn of Archean crust in the east Pilbara Craton, Western Australia: driving mechanisms and tectonic implications. *J. Struct. Geol.* **20**, 1405-1424.
- DEER, W.A., HOWIE, R.A. & ZUSSMAN, J. (1994): *An Introduction to the Rock-Forming Minerals* (2nd ed.). Longman Limited, London, U.K.
- DROOP, G.T.R. (1989): Reaction history of garnet–sapphirine granulites and conditions of Archean high-pressure granulite-facies metamorphism in the central Limpopo mobile belt, Zimbabwe. *J. Metamorph. Geol.* **7**, 383-403.
- ESSENE, E. J. (1989): The current status of thermobarometry in metamorphic rocks. In *Evolution of Metamorphic Belts* (J.S. Daly, R.A. Cliff & B.W.D. Yardley, eds.). *Geol. Soc., Spec. Publ.* **43**, 1-44.
- FUHRMAN, M.L. & LINDSLEY, D.H. (1988): Ternary-feldspar modeling and thermometry. *Am. Mineral.* **73**, 201-216.
- GOULET, N. & CADÉRON, S. (2000): Étude thermobarométrique des enclaves du Complexe de Troie. *Rapport interne, Ministère des Ressources Naturelles*.
- HARLEY, S.L. (1986): A sapphirine – cordierite – garnet – sillimanite granulite from Enderby Land, Antarctica: implications for FMAS petrogenetic grids in the granulite facies. *Contrib. Mineral. Petrol.* **94**, 452-460.
- _____ (1998): Ultrahigh temperature granulite metamorphism (1050°C, 12 kbar) and decompression in garnet (Mg₇₀) – orthopyroxene – sillimanite gneisses from the Rauer Group, East Antarctica. *J. Metamorph. Geol.* **16**, 541-562.
- _____ & MOTOYOSHI, Y. (2000): Al zoning in orthopyroxene in a sapphirine quartzite; evidence for >1120°C UHT. *Contrib. Mineral. Petrol.* **138**, 293-307.
- HENSEN, B. J. (1987): *P–T* grids for silica-undersaturated granulites in the system MAS (n + 4) and FMAS (n + 3) – tools for the derivation of *P–T* paths and metamorphism. *J. Metamorph. Geol.* **5**, 255-271.
- _____ & HARLEY, S.L. (1990): Graphical analysis of *P–T–X* relations in granulite facies metapelites. In *High Temperature Metamorphism and Crustal Anatexis* (J.R. Ashworth & M. Brown, eds.). Unwin-Hyman, London, U.K. (19-56).
- HERD, R. (1991): An update on the occurrence of sapphirine-bearing assemblages in Canada, with comments on their tectonic significance. *Geol. Assoc. Can. – Mineral. Assoc. Can., Program Abstr.* **16**, 54.
- KRETZ, R. (1983): Symbols for rock-forming minerals. *Am. Mineral.* **68**, 277-279.
- MADORE, L., BANDYAYERA, D., BÉDARD, J.H., BROUILLETTE, P., SHARMA, K.N.M., BEAUMIER, M. & DAVID, J. (1999): Géologie de la région du Lac Peters (SNRC 24M). *Minist. Ress. Nat., Québec, Rapp. Géol.* **RG 99-07** (accompanies map **SI-24M-C2G-99**).
- MOHAN, A. & WINDLEY, B.F. (1993): Crustal trajectory of sapphirine-bearing granulites from Ganguvarpatti, South India; evidence for an isothermal decompression path. *J. Metamorph. Geol.* **11**, 867-878.
- NICHOLS, G.T., BERRY, R.F. & GREEN, D.H. (1992): Internally consistent gahnitic spinel – cordierite – garnet equilibria in the FMASHZn system: geothermobarometry and applications. *Contrib. Mineral. Petrol.* **111**, 362-377.
- NIJLAND, T.G., TOURET, J.L.R. & DIEDERIK, V. (1998): Anomalous low temperature orthopyroxene, spinel, and sapphirine occurrences in metasediments from the Bamble amphibolite-to-granulite facies transition zone (South Norway): possible evidence for localized action of saline fluids. *J. Geol.* **106**, 575-590.
- OWEN, J.V. & GREENOUGH, J.D. (1991): An empirical sapphirine–spinel Mg–Fe exchange thermometer and its application to high grade xenoliths in the Popes Harbour dyke, Nova Scotia, Canada. *Lithos* **26**, 317-332.
- PERCIVAL, J.A., MORTENSEN, J.K., STERN, R.A., CARD, K.D. & BÉGIN, N.J. (1992): Giant granulite terranes of northeastern Superior Province: the Ashuanipi Complex and Minto Block. *Can. J. Earth Sci.* **29**, 2287-2308.
- _____ & SKULSKI, T. (2000): Tectonothermal evolution of the northern Minto block, Superior Province, Quebec, Canada. *Can. Mineral.* **38**, 345-378.

- _____, _____ & NADEAU, L. (1997): Reconnaissance geology of the Pelican–Nantais Belt, northeastern Superior Province, Quebec. *Geol. Surv. Can., Open-File Map* **3525** (scale 1:250,000).
- _____, STERN, R.A. & SKULSKI, T. (2001): Crustal growth through successive arc magmatism, northeastern Superior Province, Canada. *Precamb. Res.* **109**, 203-238.
- _____, _____, _____, CARD, K.D., MORTENSEN, J.K. & BÉGIN, N.J. (1994): Minto block, Superior Province: missing link in deciphering assembly of the craton at 2.7 Ga. *Geology* **22**, 839-842.
- PODLESSKII, K.K. & KURDYUKOV, Y.B. (1992): The association sapphirine + quartz in the Chogar and Sharyzhalgay complexes, east Siberia. *Int. Geol. Rev.* **34**, 611-616.
- SPEAR, F.S. (1993): *Metamorphic Phase Equilibria and Pressure–Temperature–Time Paths*. Mineralogical Society of America, Washington, D.C.
- VIELZEUF, D. (1983): The spinel and quartz associations in the high grade xenoliths from Tallante (S.E. Spain) and their potential use in geothermometry and barometry. *Contrib. Mineral Petrol.* **82**, 301-311.

Received July 14, 2002, revised manuscript accepted December 15, 2004.